Neutrino-induced showers in the ANTARES Deep-Sea Telescope

Q. Dorosti Hasankiadeh*, H. Löhner,
on behalf of the ANTARES Collaboration

KVI, University of Groningen, Zernikelaan 25, NL-9747 AA Groningen, The Netherlands

Abstract

Reconstruction of neutrino-induced showers, initiated by neutral-current interactions, can extend the sensitivity of the ANTARES detector to all neutrino flavors. A major challenge in reconstructing showers is their selection from an overwhelming background of down-going atmospheric muons. We have developed a shower selection strategy in order to select up-going showers with high efficiency and purity. We have tuned the selection strategy on Monte-Carlo simulations containing the proper amount of background and atmospheric neutrino-induced showers. The obtained results indicate an efficiency of 21% with a purity better than 90% for the shower selection. We applied the selection strategy to ANTARES experimental data and observed a satisfactory performance of the discriminating variables.

Keywords: Neutrino-induced shower, ANTARES, shower selection strategy
PACS: 95.55.Vj

1. Introduction

ANTARES [1] is the largest neutrino telescope operating in the northern hemisphere and is located roughly 40 km off the south coast of France in the Mediterranean Sea. ANTARES aims to search for high-energy neutrinos originating from galactic and extra-galactic sources. The detection principle relies on the measurement of Cherenkov light emitted from up-going relativistic charged particles caused by the interaction of neutrinos with matter inside or surrounding the active detection volume. The Earth is exploited as a filter and thus the overwhelming amount of down-going atmospheric muons can be reduced. In order to achieve a high angular resolution, the ANTARES data analysis was primarily focused on the reconstruction of muon tracks produced in charged-current interactions of muon neutrinos. Nevertheless, charged-current interactions of electron and τ neutrinos as well as neutral-current interactions of all neutrino flavors can cause hadronic showers. Thus, the reconstruction of showers can extend the sensitivity of ANTARES to all neutrino flavors, which can furnish measurements of the neutrino-flavor ratio. The expected standard neutrino-flavor ratio on Earth, $\nu_e : \nu_\mu : \nu_\tau = 1 : 1 : 1$, assuming neutrino production through the decay of charged pions caused by interactions of high energy protons with photons or nucleons [2] and taking into account neutrino oscillations. Any observed deviation from the standard neutrino-flavor ratio can either provide constraints on astrophysical models [3], or probe for new physics [2, 4]. Moreover, the reconstruction of neutrino-induced showers would allow a more precise neutrino-energy measurement compared to that of muon tracks, since showers release their entire energy in a compact region inside the active detection volume. This property is particularly important for diffuse-flux studies. On the other hand, due to the short length of showers, the resolution of the direction reconstruction of showers is deteriorated. Consequently, the identification of showers within the down-going atmospheric muon background critically challenges the efficiency of any shower-selection strategy [5]. Altogether, it is crucial to identify neutrino-induced showers with high efficiency and purity.

2. Shower selection strategy

For hadronic showers resulting from neutrino interactions in the energy range detected with a deep-sea telescope like ANTARES the typical shower length is about 10 m which is about 100 times shorter than the length of muon tracks. This deteriorates the sensitivity for shower events by a factor of 5, since only those neutrino-induced showers interacting in the active volume can give rise to the detection, whereas muons can travel through several kilometers of water toward the detector [6]. Despite the disadvantage of the inherently poor angular resolution of showers, their shorter length, however, can be exploited as a signature to separate them more efficiently from the muon background. We have developed a shower selection strategy based on a sequence of discriminating criteria. First, we suppress the atmospheric muon background by estimating the shower direction from the directions of light emission and rejecting down-going events as well as selecting events with sufficient charge deposition as measured by the total number of photo electrons (pe's) collected by the photo sensors for this event. Subsequently, we reconstruct the shower vertex by exploiting the causality relation for the propagation of Cherenkov

*Corresponding author
Email address: q.dorosti.hasankiadeh@rug.nl (Q. Dorosti Hasankiadeh)

light emitted from shower particles, approximating showers as point-like objects. By combining various quality cuts on observables describing the shower structure, we are able to improve the signal to background ratio considerably at the expense of a shower selection efficiency of about 21%.

2.1. Monte Carlo and experimental samples

In order to apply the strategy on ANTARES experimental data, we tuned the selection criteria on Monte-Carlo (MC) simulated events. The simulation chain [7, 8] produces neutrino-induced secondary particles and down-going atmospheric muons. It includes the generation of Cherenkov light, digitization of photo sensor signals (hits), simulation of the triggers and optical background caused by the decay of ^{40}K and bioluminescence. Neutrino-induced shower events, corresponding to the live time of a year, were generated in the neutrino energy range $10^2 \leqslant E \leqslant 10^7$ GeV with a power-law energy spectrum decreasing as E^{-2} and zenith angle of $0° \leqslant \theta \leqslant 180°$, where vertically "down-going" corresponds to $\theta = 180°$. Further, an energy-dependent weighting factor was applied to produce a spectrum of conventional atmospheric neutrinos from the charged meson decay [9]. In order to test the performance of our shower selection strategy, we used a fraction of experimental data, taken in 2010, with a total live time of 86.4 hours. Atmospheric muons with the equivalent live time were simulated with the MUPAGE package [10] and the neutrino-induced showers were scaled down to the equivalent live time. In order to suppress the optical background, we selected hits which fulfill the condition of a loose ANTARES trigger ("3N") which requires at least 5 hits distributed on 2 detection lines and appearing in a certain coincidence-time window.

2.2. Up-going selection

The number of detected atmospheric muons at the ANTARES site is in the order of a few hundred million events/year [11], which can be about 5–6 orders of magnitude higher than the expected number of detected atmospheric neutrino-induced showers per year. In order to reject the down-going muon background, one can apply a direction reconstruction method to select only up-going events. However, the intrinsically poor angular resolution of showers requires a reconstruction algorithm which is efficient for both showers and muon tracks. Therefore, as schematically shown in Fig. 1, we developed an algorithm, called Light Direction, which estimates the direction of events by calculating the direction of the light emission vector, $\vec{D}$. In Fig. 1, the passage of a hypothetical down-going muon through four detection lines is shown (dashed arrow). The emitted Cherenkov light hits a certain number of photo sensors (filled circles). Then the Light Direction is defined as the mean of the light vectors $\vec{D}_i$, which connect the earliest of the N hits to all other N-1 hits:

$$\vec{D} = \frac{1}{N-1} \sum_{i=1}^{N} \vec{D}_i \qquad (1)$$

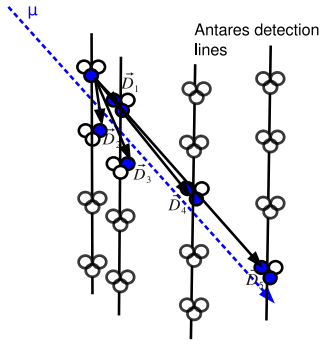

Figure 1: Sketch of the principle of the Light Direction method. Displayed: the passage of the hypothetical down-going muon (dashed arrow), hit photo sensors (filled circles) and light vectors (solid arrows) $\vec{D}_i$.

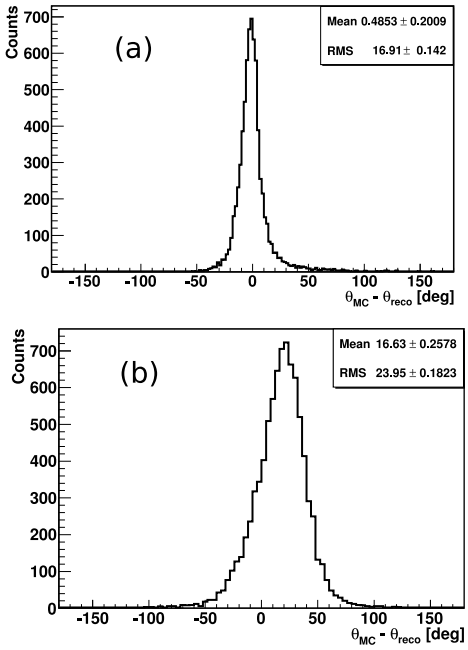

Figure 2: Performance of the Light Direction method for the MC samples of down-going atmospheric muons (a) and of showers (b). Shown are the differences between the true MC θ and reconstructed θ angles.

The performance of the Light Direction method on the MC sample of down-going atmospheric muons and that of showers is shown in Fig. 2 (a) and (b), respectively, where the difference between the true MC zenith angles θ and the reconstructed ones is plotted. The spread of the θ angle distribution is about 17° for atmospheric muons and 24° for showers. The positive offset in Fig. 2 (b) indicates the preference of the algorithm to reconstruct up-going showers, which is caused by the downward orientation of the ANTARES photo sensors. Consequently, any up-going event selection ($\theta < 90°$) mostly preserves all up-going showers. Applying only the Light Direction method on the MC atmospheric muon background by slecting up-going events ($\theta < 90°$) provides a background rejection by merely a factor of 21. In order to suppress the remaining mis-reconstructed atmospheric muons, we combined

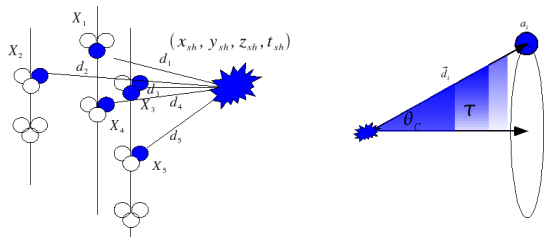

Figure 3: Sketch of a hypothetical point-like shower. Left: the space-time position $\vec{X_{sh}}$ of the shower producing 5 hits (filled circles) at distances of d_i's from the shower vertex. Right: a shower light cone, under the Cherenkov angle of θ_C, hitting a photo sensor with the measured hit amplitude a_i at distance d_i from the shower position.

the Light Direction with BBFit, an algorithm for muon track reconstruction [12], such that we select only the events which are reconstructed as up-going by both methods. This combination of BBFit and Light Direction allows an atmospheric muon suppression by a factor of 116 (Cut 1 in Table 1).

2.3. Shower vertex reconstruction

To reconstruct the shower vertex, we exploit the causality relation for the propagation of Cherenkov light emitted from a point-like source. The detection of a hypothetical point-like shower is schematically shown in Fig. 3, where the shower interacts at the space-time position of $\vec{X_{sh}} = (x_{sh}, y_{sh}, z_{sh}, (c/n)t_{sh})$. The light emitted from the shower fires a certain number of photo sensors (filled circles) with measured space-time coordinates of $\vec{X_i} = (x_i, y_i, z_i, (c/n)t_i)$, where c/n is the velocity of light in water with the refraction index of n. For a perfectly point-like shower, the time difference ΔT between the measured hit time and the expected photon travel time from the shower vertex must be equal to zero.

$$\Delta T = \left(\frac{n}{c}d_i + t_{sh}\right) - t_i = 0, \quad i = 1, 2, ..., N, \tag{2}$$

where $d_i = \sqrt{(x_{sh} - x_i)^2 + (y_{sh} - y_i)^2 + (z_{sh} - z_i)^2}$ is the distance of the hit photo sensor i from the shower vertex and N is the number of hits. To efficiently reconstruct the vertex, we split the algorithm into the two following steps:

Step 1: we estimate the mean space-time position of the shower by analytically solving the above set of N equations for the four unknown coordinates of $\vec{X_{sh}}$. A pairwise subtraction of the equations cancels out the squares of the components of X_{sh} and then the $\vec{X_{sh}}$ can simply be calculated by solving $N - 1$ linear equations [6]:

$$\vec{X_{sh}} = A^{-1} \cdot \vec{b}, \tag{3}$$

where A is a $(N - 1) \times 4$ matrix with the components:

$$a_{jk} = 2(\vec{X_{j+1}} - \vec{X_j})_k, \quad k = 1, 2, 3, 4 \tag{4}$$

and k corresponds to the four space-time positions of the shower and $\vec{b}$ is a vector with the components:

$$b_j = X_{j+1}^2 - X_j^2, \tag{5}$$

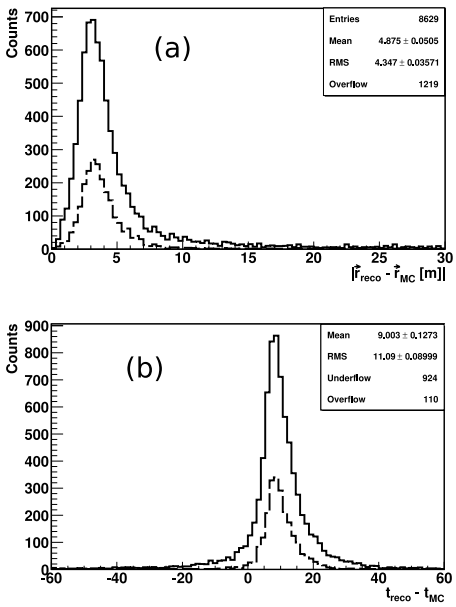

Figure 4: Performance of the reconstruction algorithm for the shower-interaction vertex position (a) and the shower time (b). Dashed lines show the performance of the algorithm after the purity cuts (Section 3.2).

with $j = 1, ..., N - 1$. We can define the residual parameter $R = |\vec{X_{sh}} - A^{-1} \cdot \vec{b}|$, which judges how well the event looks like a point source of light.

Step 2: we apply an M-estimator of the following form which minimizes ΔT in order to estimate the best value for $\vec{X_{sh}}$:

$$M = 2 \times \sqrt{1 + \frac{\Delta T^2}{2\sigma^2}} - 2, \tag{6}$$

where σ is the ANTARES time measurement error which is 1 ns [1]. The above M-estimator function is chosen to be less sensitive to outliers which cause some fluctuations in the error estimation [13]. The results of Step 1 provide starting values for the M-estimator. The performance of the algorithm of the reconstruction of the shower vertex position and the interaction time on the MC shower sample is shown in Fig. 4 (a) and (b), respectively. The distributions exhibit a spread of 4.4 m for the shower vertex and 11.1 ns for the interaction time reconstruction. The offset seen in the shower time reconstruction is due to the fact that the shower light is continuously produced in the shower depth and not exactly at the shower interaction vertex. The finite travel time of shower particles with velocity above the Cherenkov threshold always causes a positive time shift and, therefore, a related shift in the vertex reconstruction, which is consistently observed in all three spatial coordinates. In Section 3.2 we shall apply the R and M-estimator fit-quality parameters as the shower observables to identify showers within the remaining mis-reconstructed atmospheric muon background.

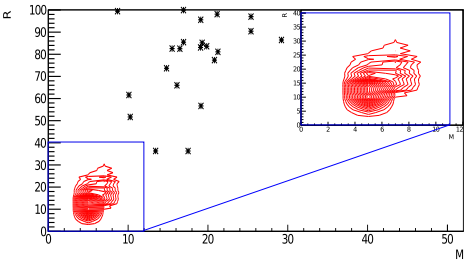

Figure 5: Distribution of shower selection variables R and M for the MC showers (red/gray contours) and mis-reconstructed up-going atmospheric muons (stars). The insert shows the expanded shower region.

3. Preliminary results

3.1. Energy reconstruction

The algorithm to reconstruct the energy of the neutrino-induced showers follows the idea that the reconstructed hit amplitude $A[pe]$ in units of photo electrons, i.e. the sum of all hit amplitudes corrected according to the light absorption length τ is correlated to the shower energy. Thus, the relation between $A[pe]$ and the hit amplitudes $a_i[pe/m]$ measured at the respective distance $d_i[m]$ from the shower vertex (Fig. 3, right) is given by:

$$A[pe] = \sum_{i=1}^{N} a_i \; d_i \; \sin(\theta_C) \; \exp(d_i/\tau), \tag{7}$$

where N is the number of hits, θ_C is the Cherenkov angle in water and the factor $\exp(d_i/\tau)$ is included to correct for the light attenuation in water. A polynomial fit to the profile distribution of the true MC shower energy vs. $A[pe]$ yields the following relation:

$$\begin{aligned} \log_{10} E_{reco}[GeV] \quad &= 0.08 \; (\log_{10} A[pe])^2 \\ &+ 0.1 \; \log_{10} A[pe] + 1.3, \end{aligned} \tag{8}$$

where E_{reco} is the reconstructed energy of showers in GeV. The algorithm results in an energy resolution of a factor of 2.2 on the shower energy.

3.2. Purity cuts on observables

We tuned the shower selection on the MC samples, described in Section 2.1. The selection strategy follows three criteria:
Cut 1: Showers must be reconstructed as up-going: $\theta < 90^\circ$ by both the Light Direction method and the BBFit method.
Cut 2: The total deposited charge per event must be more than 100 *pe*. This removes many atmospheric muons which cause a few hits and mimic a shower-like event.
Cut 3: The parameters R < 40 and M < 11 are required, which are optimized to remove the remaining muon background, as shown in Fig. 5.
All the events falling into the shower region (Fig. 5, R < 40 and M < 11) are selected as showers, which corresponds to a selection efficiency of 21% and a selection purity higher than 90%. The number of reconstructed experimental events in the live time of 86.4 hours and the corresponding MC simulation events after each cut are summarized in Table 1. The obtained results indicate one shower-like event during the live time, whereas according to the simulation, 0.5 shower events are expected. The distributions of the M-estimator fit quality parameter show good agreement between the experimental data and the MC simulation.

Table 1: Number of measured events in 86.4 hours of data taking and the equivalent number of simulated MC events for atmospheric neutrino-induced showers and atmospheric muon tracks.

	MC μ_{Atm}	MC ν_{shower}	Experimental data
Reco	905265	2.4	961948
Cut 1	7805	1.8	8978
Cut 2	434	0.63	400
Cut 3	0	0.5	1

4. Summary

ANTARES primarily aims to reconstruct neutrino-induced muons. Nevertheless, the reconstruction of neutrino-induced showers can protrude the sensitivity to all neutrino flavors, allowing for a measurement of the neutrino-flavor ratio. We have developed a method to largely suppress the huge background and reconstruct showers by combining quality cuts on the observables describing the shower structure. We adjusted the selection strategy using MC events. The applied strategy selects showers with an efficiency of 21% and a purity higher than 90%. Moreover, we applied the selection strategy on a fraction of ANTARES experimental data with live time of 86.4 hours. The distribution of the M-estimator fit-quality parameter of the MC simulations fairly well coincides with that of the experimental data. The shower selection strategy will be applied to a large experimental data sample and be used to study the physics related to the neutrino-induced showers.

5. References

[1] M. Ageron et al., Nucl. Instrum. Meth. A 656 (2011) 11-38; arXiv:1104.1607v2.
[2] J.G. Learned and S. Pakvasa, Astropart. Phys. 3, 267 (1995).
[3] T. Kashti, E. Waxman, Phys. Rev. Lett. 95 (2005) 181101.
[4] H. Athar, M. Jezabek, and O. Yasuda, Phys. Rev. D 62, 103007 (2000).
[5] F. Folger. *Reconstruction of neutrino induced hadronic showers with the ANTARES neutrino telescope.* Diploma thesis, University of Erlangen-Nuremberg, Germany, 2009.
[6] B. Hartmann. *Reconstruction of Neutrino-Induced Hadronic and Electromagnetic showers with the ANTARES Experiment.* PhD thesis, University of Erlangen-Nuremberg, Germany, 2006.
[7] J. Brunner. *Antares simulation tools.* 1st VLVnT Workshop, Amsterdam, The Netherlands, 5-8 Oct 2003. http://www.vlvnt.nl:/proceedings/
[8] J.A. Aguilar et al., Astropart. Phys. 34 (2010) 179.
[9] G.D. Barr, T.K. Gaisser, P. Lipari, S. Robbins, and T. Stanev, Phys. Rev. D70 (2004) 023006.
[10] Y. Becherini, A. Margiotta, M. Sioli and M. Spurio, Astropart. Phys. 25 (2006) 1; G. Carminati, M. Bazzotti, A. Margiotta, and M. Spurio. Comp. Phys. Comm., 179 (2008) 915.
[11] J.A. Aguilar et al., Phys. Lett. B696 (2011) 16-22, arXiv:1011.3772.
[12] J.A. Aguilar et al., Astropart. Phys. 34 (2011) 652-662, arXiv:1105.4116.
[13] Z. Zhang, Image and Vision Computing Journal 15 (1997) 59.